Online Resource 1

Supplementary Figures S1-S13

A multi-component herbal formulation limits PRRSV replication and reduces PD-L1-high neutrophil abundance in porcine lungs

Jintao Peng1, 2,*, Xu Wang1, 2,*, Wei Zhou1, 2, Xin Fan1, 2, Dishi Chen1, 2, Shijie Li1, 2, Pinpin Chen1, 2, Hongxia Ding1, 2, Deshi Shi1, 2, Zutao Zhou1, 2, Fangping Zhang4, Yuncai Xiao1,2,3

1 National Key Laboratory of Agricultural Microbiology, Huazhong Agricultural University, Wuhan 430070, China.
2 College of Veterinary Medicine, Huazhong Agricultural University, Wuhan 430070, China.
3 Key Laboratory of Preventive Veterinary Medicine in Hubei Province, Huazhong Agricultural University, Wuhan 430070, China.
4 Fujian Aonong Biological Technology Group Incorporation Limited

Correspondence: xyc88@mail.hzau.edu.cn (Y.X.); zfp0632@163.com (F.Z.)

Journal: Veterinary Research Communications

Contents

Fig. S1	**UMAP and quality control**
Fig. S2	**Viral-entry receptors, interferon-stimulated gene responses, and macrophage ISG rescue**
Fig. S3	**Neutrophil subcluster details**
Fig. S4	**T-cell full panel**
Fig. S5	**CellChat focus plots for MIF–CD74/CD44 (A) and PD-1/PD-L1 (B) signaling in PRRSV-infected and APRR-treated lungs**
Fig. S6	**CellChat and ISG supporting plots**
Fig. S7	**SCENIC identifies regulons reshaped by APRR**
Fig. S8	**Cell proportion pies**
Fig. S9	**Pathway activity by ssGSEA**
Fig. S10A	**Network pharmacology convergence of in-blood APRR constituents onto pig-validated core targets and mechanism modules**
Fig. S10B	**Flow of annotated APRR constituents from the whole formula to serum, target class and mechanism module**
Fig. S10C	**Chemical profile of APRR by HPLC-MS**
Fig. S11	**Module-score heatmaps**

Figure legends are reproduced on the page carrying each figure. This file is cited in the manuscript as Online Resource 1.

Fig. S1

Online Resource 1

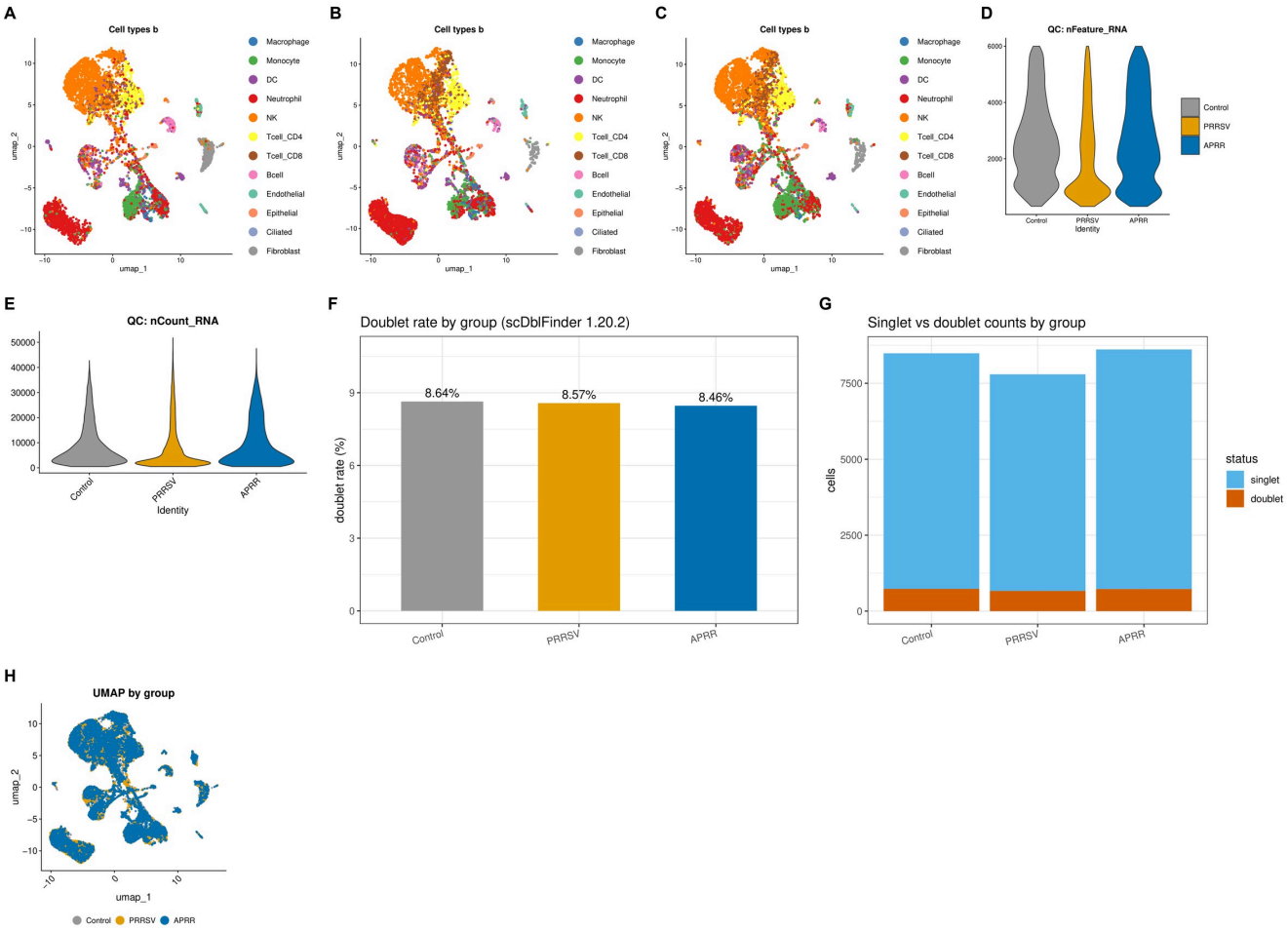


Fig. S1 UMAP and quality control. (A) UMAP of lung cells from the Control group colored by cell type. (B) UMAP of the PRRSV group. (C) UMAP of the APRR group. (D) QC metric: number of features per cell. (E) QC metric: number of counts per cell. (F) Doublet rate by group. (G) Doublet count by sample. (H) UMAP colored by group

Fig. S2

Online Resource 1

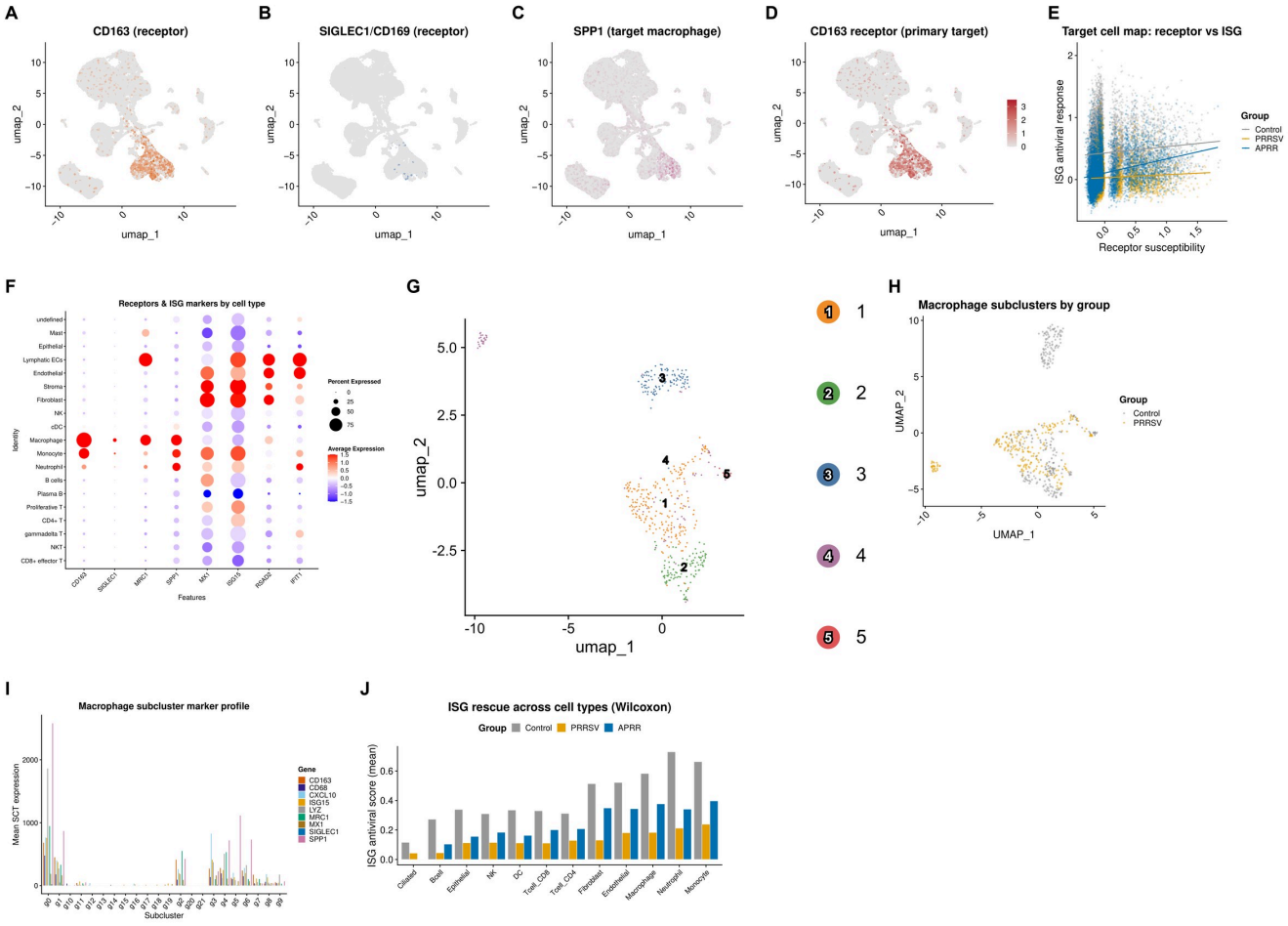


Fig. S2 Viral-entry receptors, interferon-stimulated gene responses, and macrophage ISG rescue. (A) CD163 expression. (B) SIGLEC1 expression. (C) SPP1 expression. (D) Primary receptor feature plot. (E) Receptor–target scatter. (F) Receptor–ISG dotplot across cell types. (G) Macrophage subcluster UMAP. (H) Subclusters by group. (I) Marker-expression means. (J) ISG-rescue score by group

Fig. S3

Online Resource 1

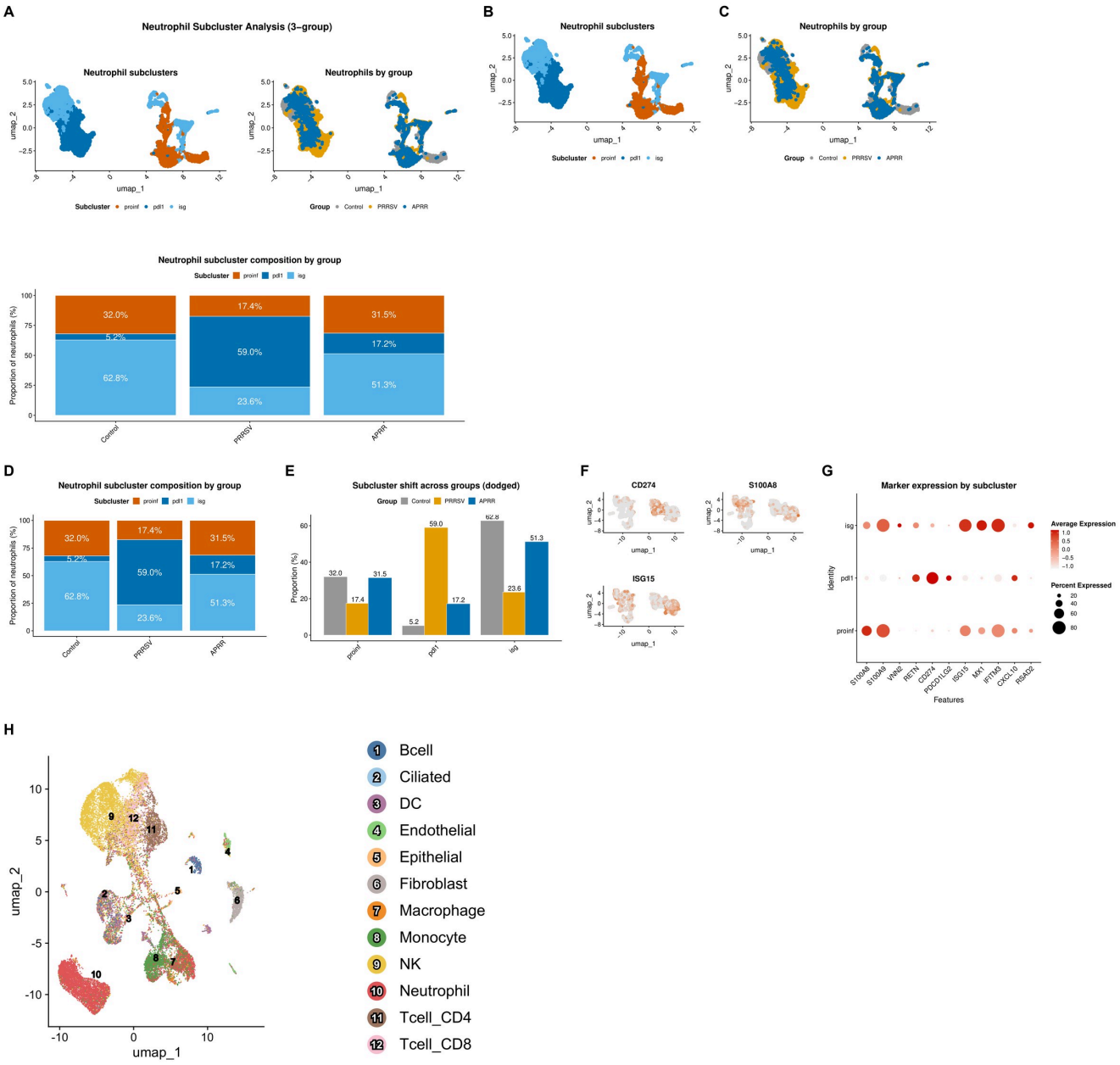


Fig. S3 Neutrophil subcluster details. (A) Combined neutrophil subcluster figure. (B) Neutrophil subcluster UMAP. (C) Neutrophil UMAP colored by group. (D) Relative proportions of neutrophil subclusters. (E) Dodge plot of subcluster proportion by group. (F) Feature plots of representative markers. (G) Subcluster dot plot. (H) Cell-type UMAP

Fig. S4

Online Resource 1

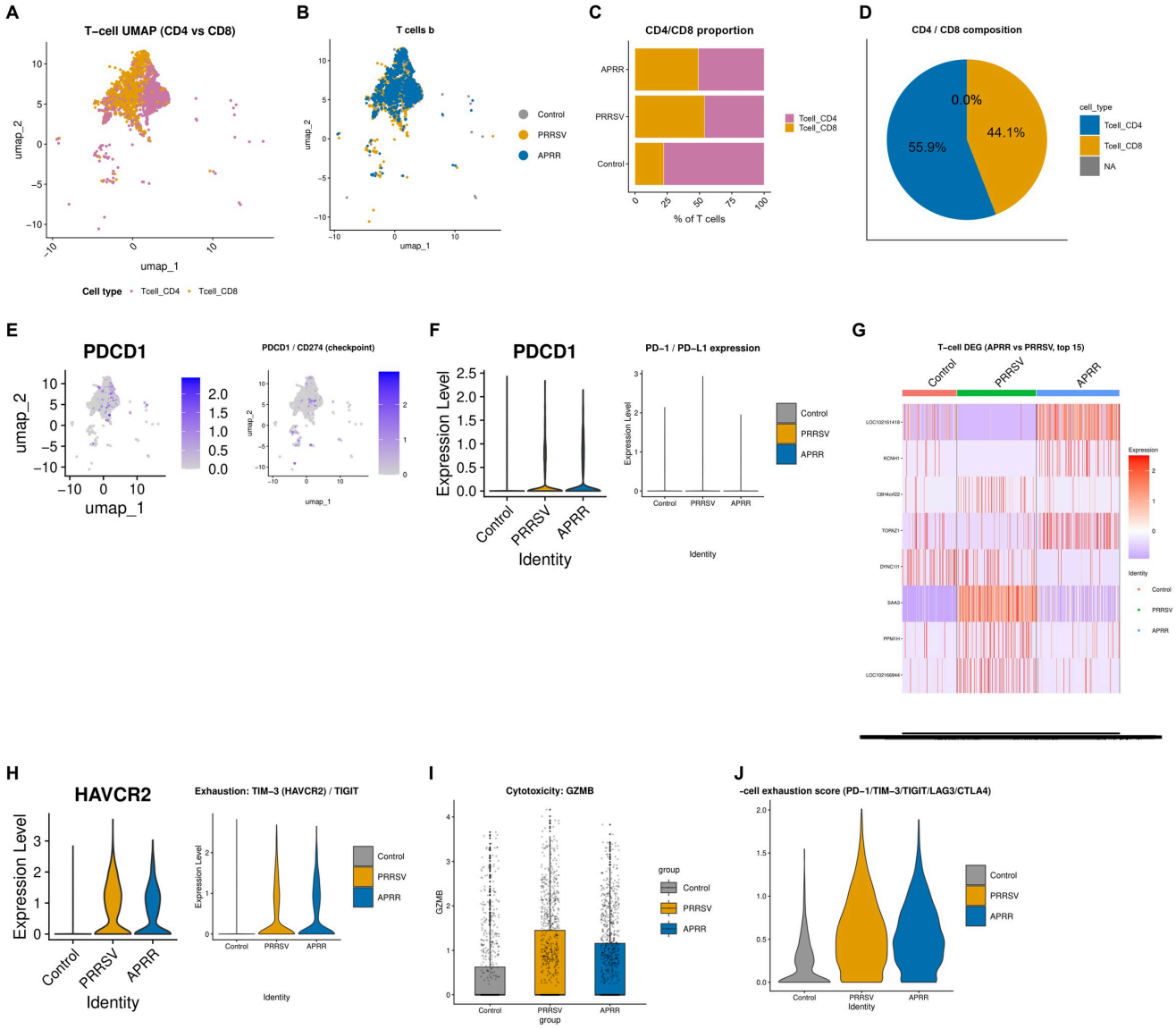


Fig. S4 T-cell full panel. (A) T-cell UMAP by cell type. (B) T-cell UMAP by group. (C) CD4⁺:CD8⁺ proportion. (D) T-cell subset pie. (E) Checkpoint-feature plot. (F) Checkpoint-gene violin. (G) T-cell DEG heatmap. (H) Exhaustion-score distribution. (I) GZMB expression. (J) Exhaustion score by group

Fig. S5

Online Resource 1

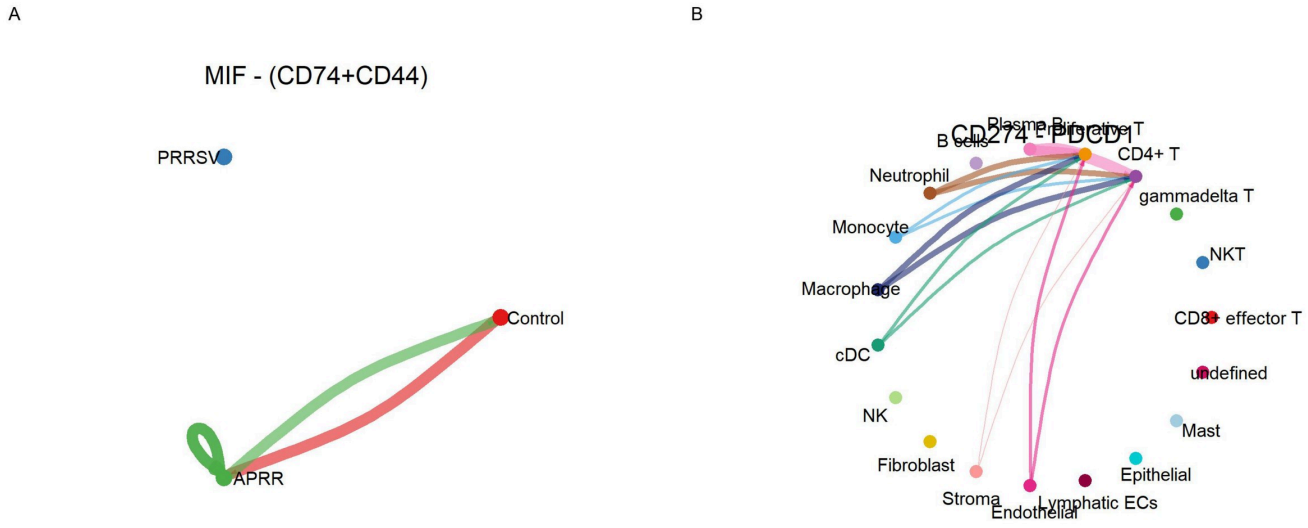


Fig. S5 CellChat focus plots for MIF–CD74/CD44 (A) and PD-1/PD-L1 (B) signaling in PRRSV-infected and APRR-treated lungs. CellChat outputs are inferred, not measured

Fig. S6

Online Resource 1

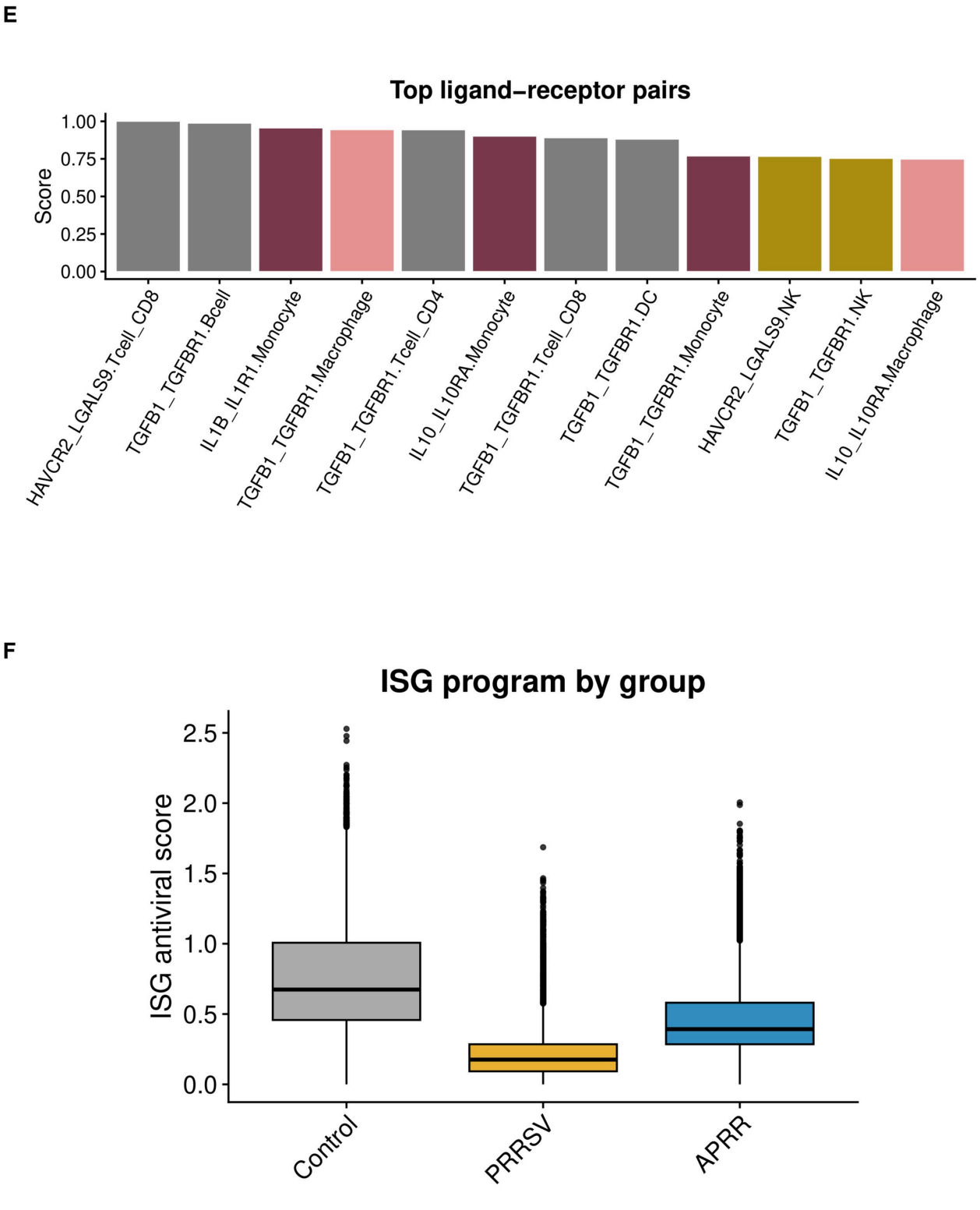


Fig. S6 CellChat and ISG supporting plots. (E) Top ligand–receptor pairs ranked by contribution. (F) ISG-expression boxplot by group. Global circle/chord/pathway/cell-type heatmaps are shown in main Fig. 6A–D

Fig. S7

Online Resource 1

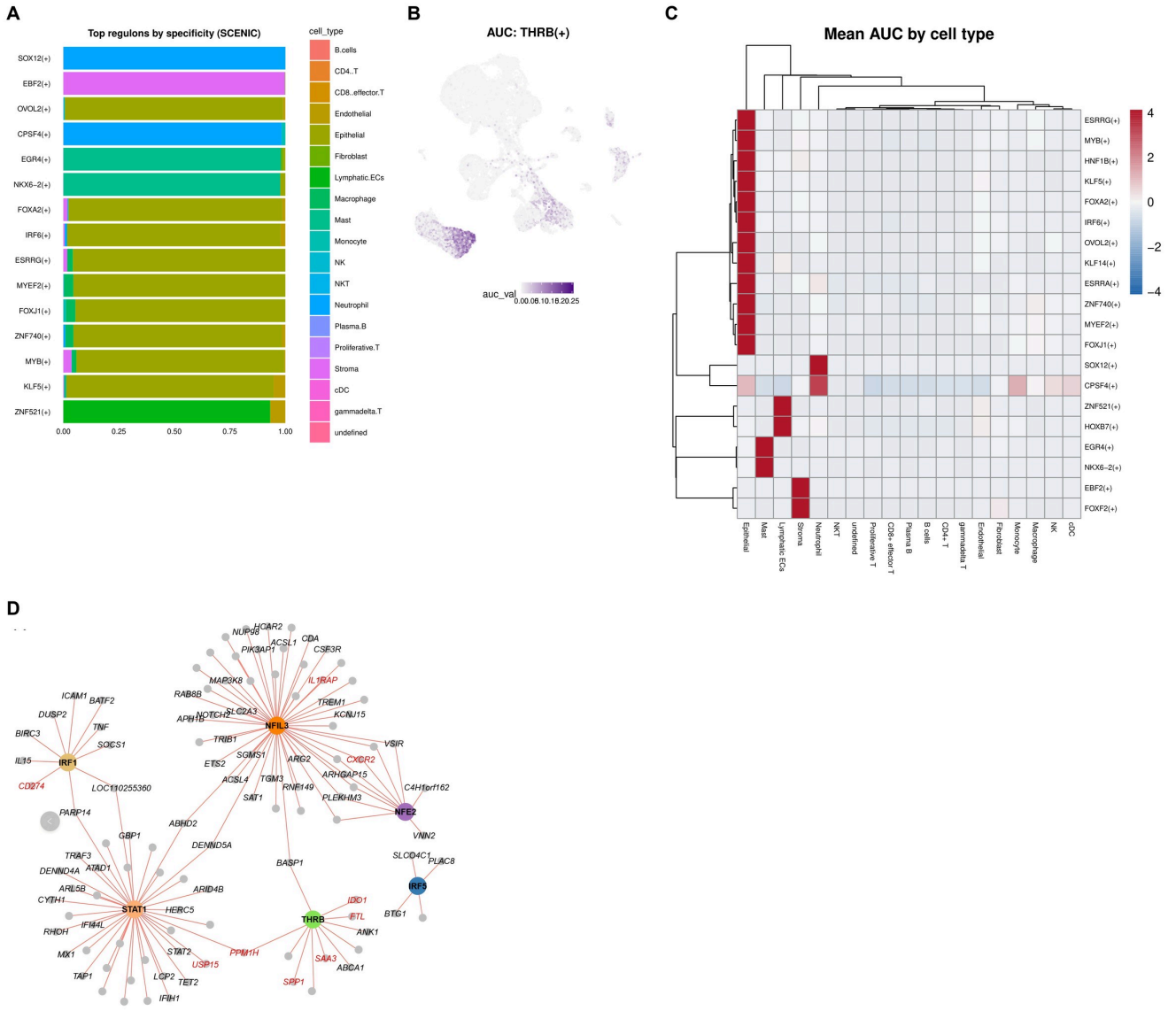


Fig. S7 SCENIC identifies regulons reshaped by APRR. (A) Regulon specificity score (RSS) of cell-type-enriched regulons. (B) AUC scores of regulon activity projected onto the UMAP across cell states. (C) Module-score heat map summarizing regulon activity per cell type. (D) Transcription factor–target network highlighting key drivers, including IRF1/STAT1-associated regulons attenuated by APRR. SCENIC was run on the three-group dataset using hg38 cisTarget rankings as a porcine proxy, as no pig-specific library is available

Fig. S8

Online Resource 1

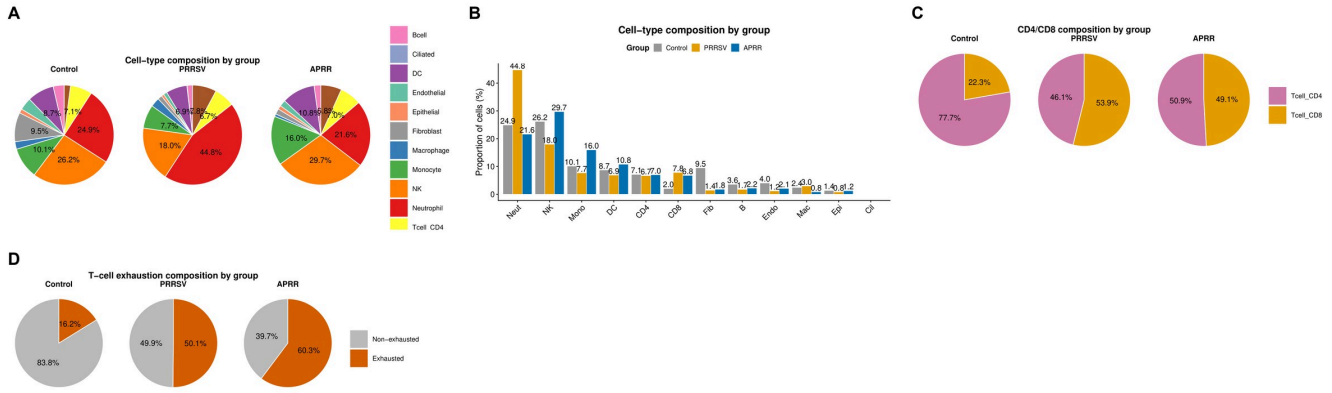


Fig. S8 Cell proportion pies. (A) Pie chart of major cell compartments across groups. (B) Highlighted neutrophil and lymphoid proportions. (C) T-cell CD4+:CD8+ pie per group. (D) T-cell exhaustion-score pie per group. Cells with an exhaustion score above the cohort median were classified as exhausted

Fig. S9

Online Resource 1

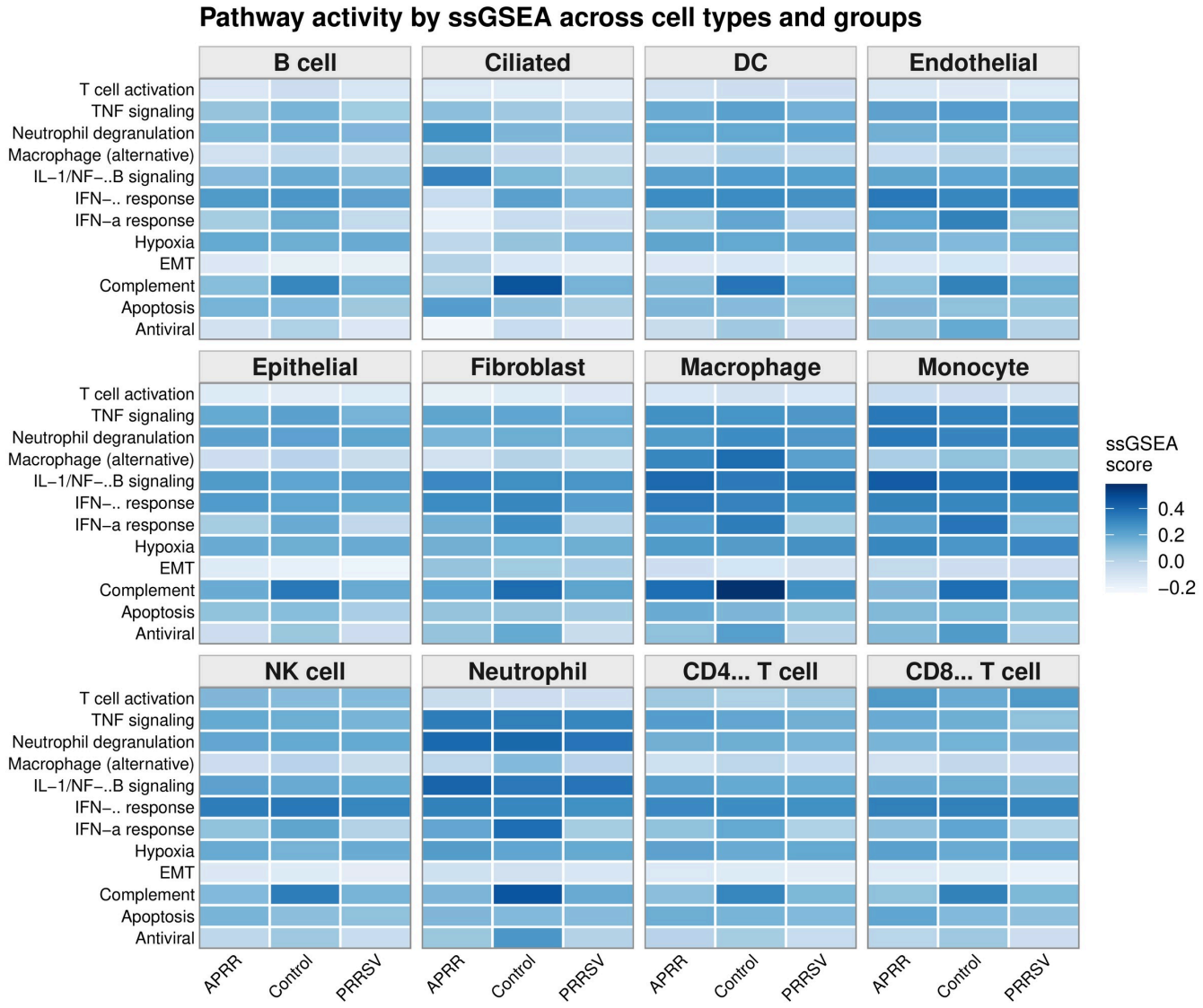


Fig. S9 Pathway activity by ssGSEA. (A) Heat map of ssGSEA scores for 12 pathways across 12 cell types and the three groups (GSVA 2.0.7, ssgsea.norm = TRUE; gene sets and versions are listed in Methods). Differential-expression KEGG enrichment of neutrophil and T-cell programs is described in the text

Fig. S10A

Online Resource 1

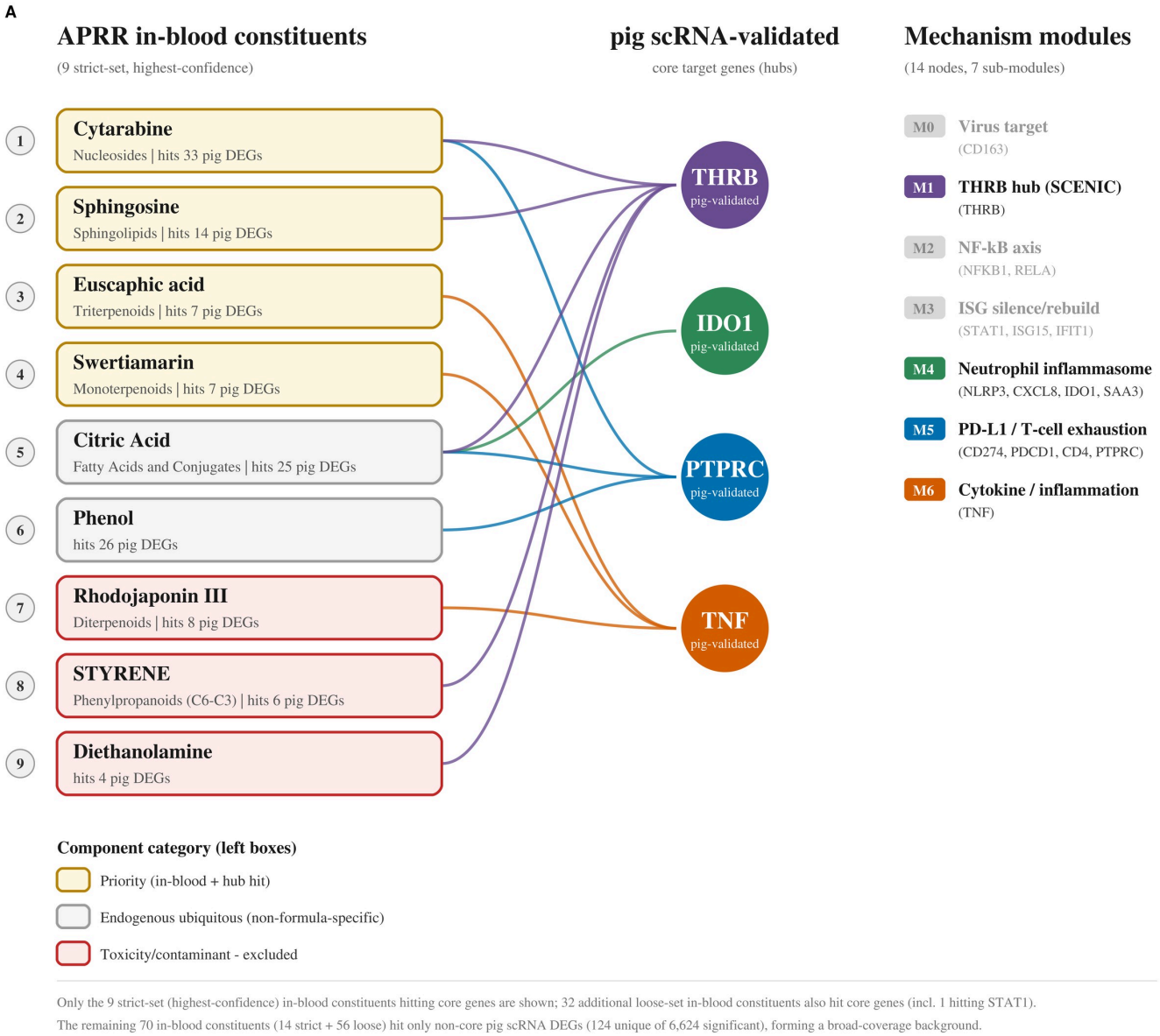


Fig. S10A Network pharmacology convergence of in-blood APRR constituents onto pig-validated core targets and mechanism modules. Left, the nine highest-confidence (strict-set) in-blood constituents detected in the serum of APRR-treated pigs, each annotated with its chemical class and the number of pig lung DEGs it hits. Centre, the pig scRNA-seq-validated core target genes (THRB, IDO1, PTPRC and TNF). Right, the 14-node mechanism modules grouped into seven sub-modules: M0 virus target (CD163), M1 THRB hub (SCENIC), M2 NF-κB axis (NFKB1, RELA), M3 ISG silencing/rebuild (STAT1, ISG15, IFIT1), M4 neutrophil inflammasome (NLRP3, CXCL8, IDO1, SAA3), M5 PD-L1/T-cell exhaustion (CD274, PDCD1, CD4, PTPRC) and M6 cytokine/inflammation (TNF). Box outline encodes constituent category: priority (in-blood plus core-gene hit), endogenous and ubiquitous (non-formula-specific), and toxicity/contaminant (excluded from interpretation). Thirty-two further loose-set in-blood constituents also hit core genes, and the remaining 70 hit only non-core pig DEGs

Fig. S10B

Online Resource 1

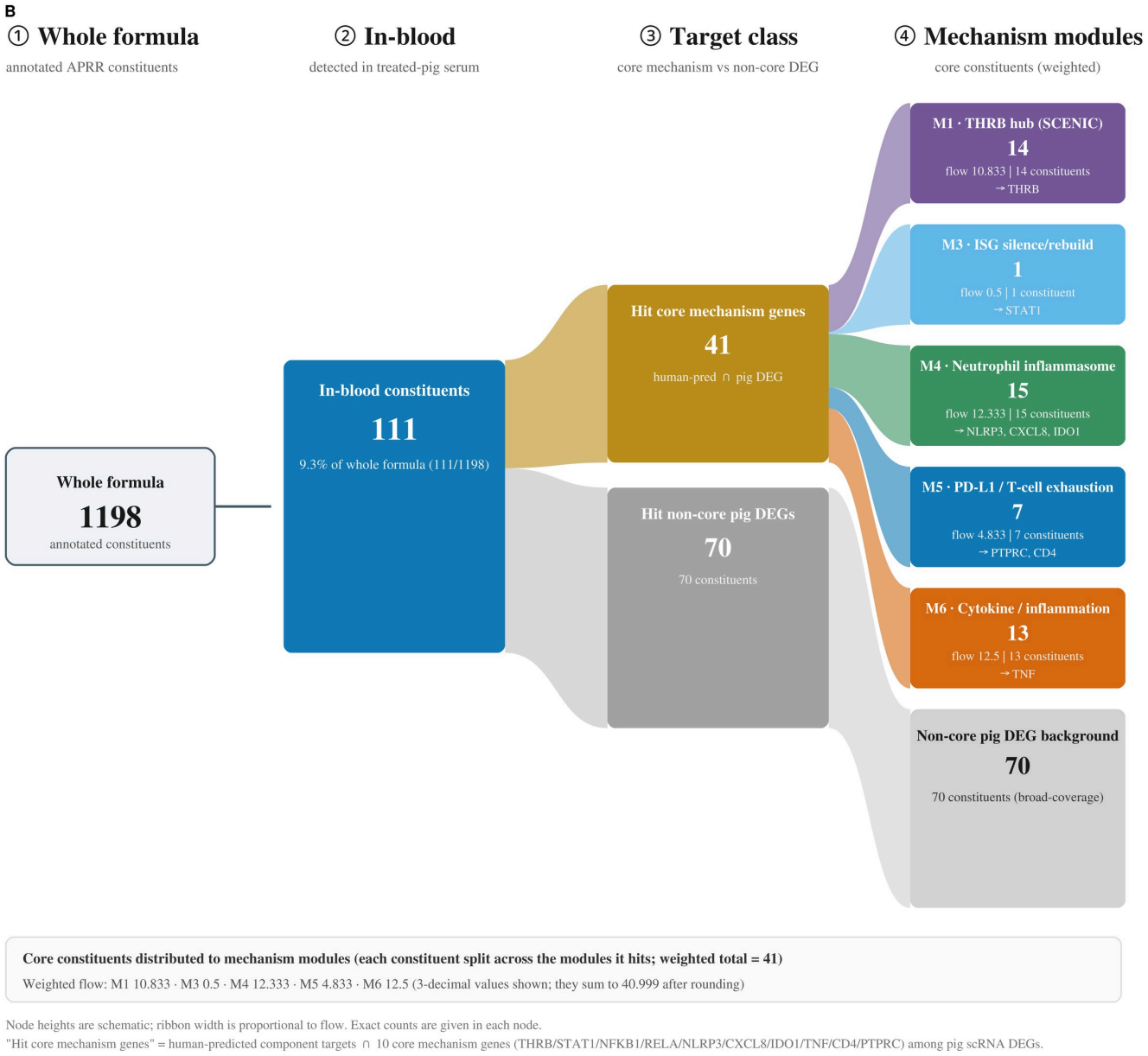


Fig. S10B Flow of annotated APRR constituents from the whole formula to serum, target class and mechanism module. Successive columns show the 1,198 annotated constituents, the 111 detected in the serum of APRR-treated pigs (9.3%), their target class (41 hitting core mechanism genes, 70 hitting only non-core pig DEGs) and the module distribution of the 41 core-hitting constituents: M1 THRB hub (14), M3 ISG silencing/rebuild (1), M4 neutrophil inflammasome (15), M5 PD-L1/T-cell exhaustion (7) and M6 cytokine/inflammation (13), giving a weighted total of 41 because constituents that hit several modules are split proportionally. Ribbon width is proportional to flow and node height is schematic; exact counts are labelled in each node

Fig. S10C

Online Resource 1

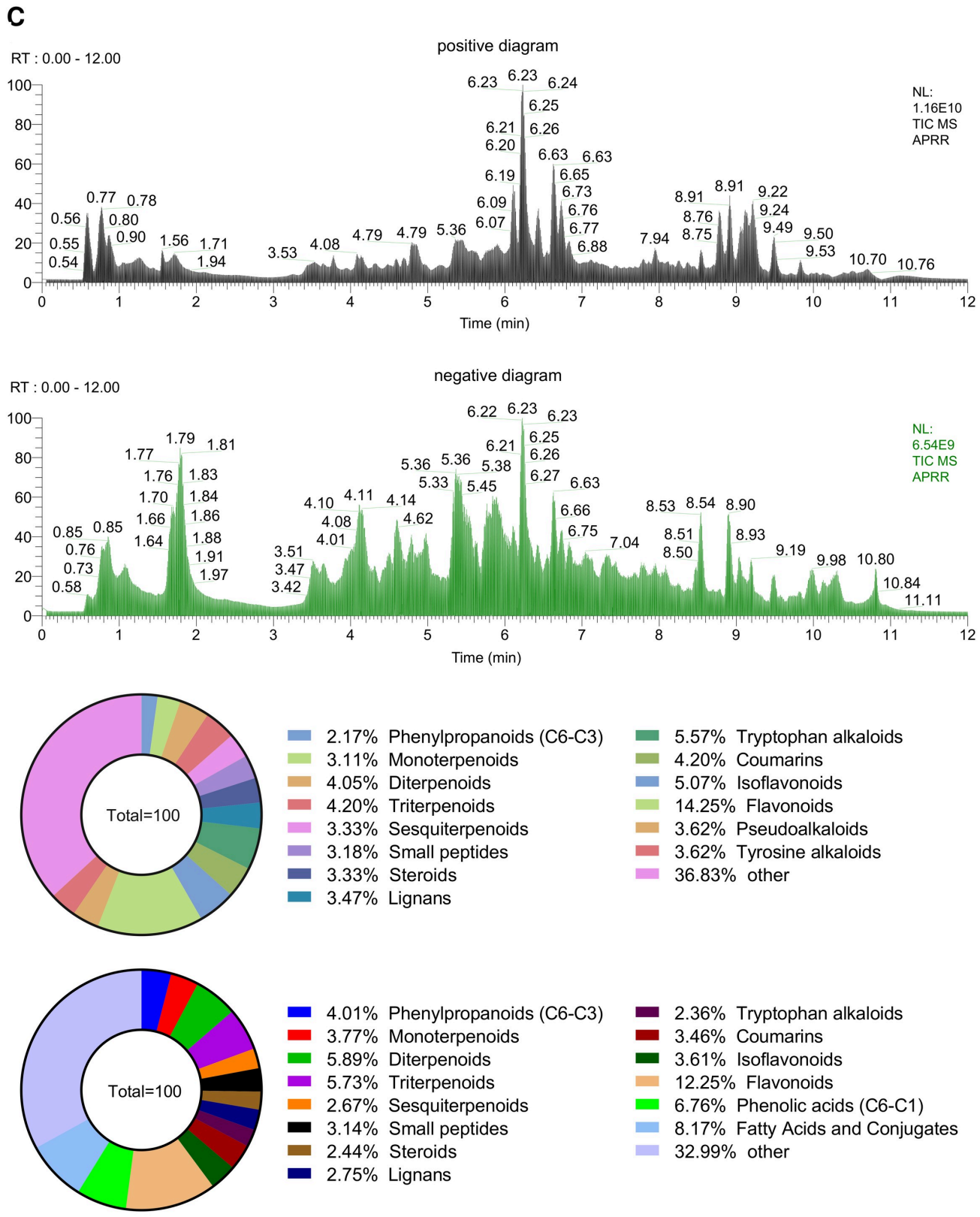


Fig. S10C Chemical profile of APRR by HPLC-MS. Total ion chromatograms in positive (upper) and negative (lower) electrospray ionization modes over 0–12 min. Ring charts summarize the annotated compound classes as a percentage of total signal for each mode; the largest annotated classes are flavonoids (14.3% positive, 12.3% negative), fatty acids and conjugates (8.2%, negative) and phenolic acids (6.8%, negative), and 36.8% (positive) and 33.0% (negative) of the signal remained unclassified

Fig. S11

Online Resource 1

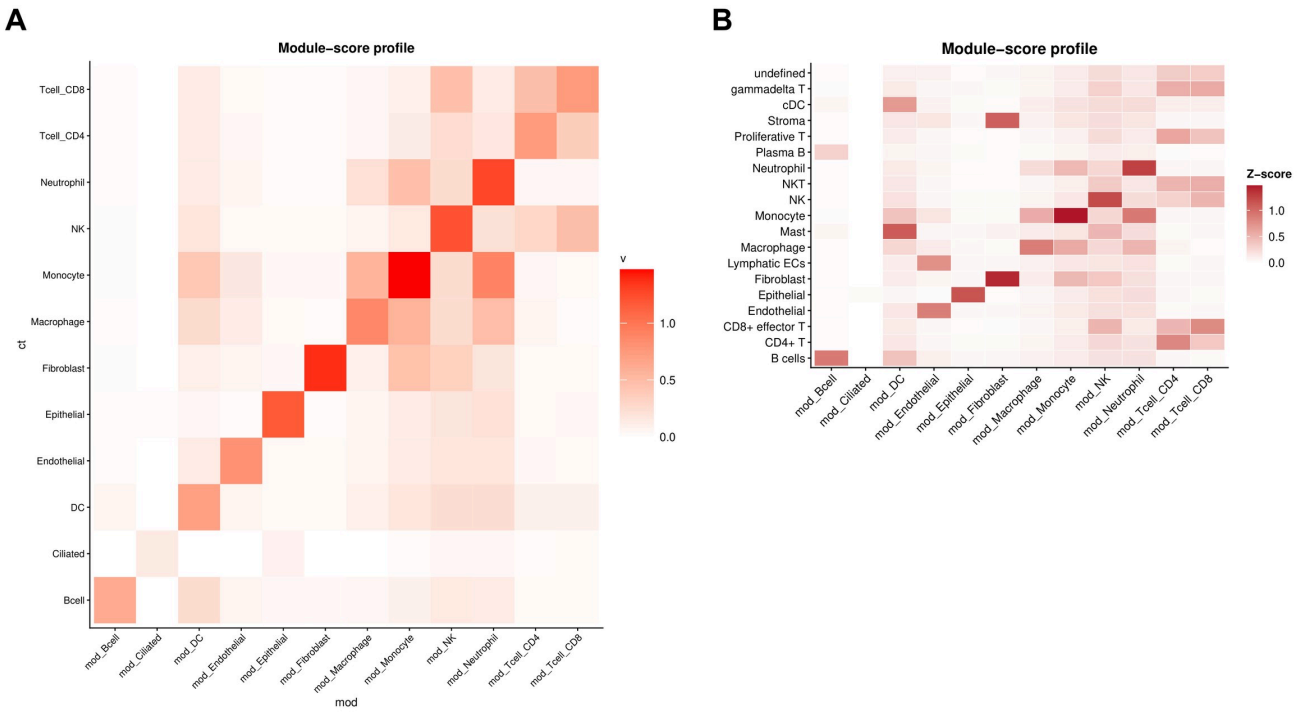


Fig. S11 Module-score heatmaps. (A) Module-score heatmap of lineage markers. (B) Module-score heatmap across cell types